Pharmacophore-Based Screening and Identification of Novel Human Ligase I Inhibitors with Potential Anticancer Activity

Shagun Krishna,[†,∥] Deependra Kumar Singh,[†,∥] Sanjeev Meena,[‡] Dipak Datta,[‡,§] Mohammad Imran Siddiqi,*[,†,§] and Dibyendu Banerjee*[,†,§]

[†]Molecular and Structural Biology Division, CSIR-Central Drug Research Institute, Lucknow 226031, India
[‡]Biochemistry Division, CSIR-Central Drug Research Institute, Lucknow 226031, India
[§]Academy of Scientific and Innovative Research, New Delhi, India

S *Supporting Information*
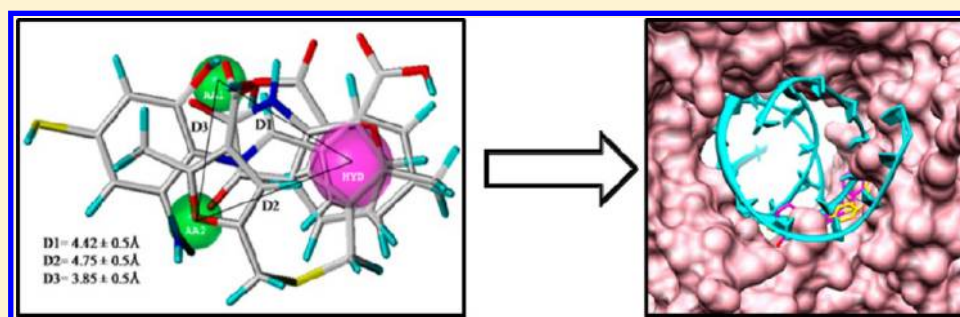
ABSTRACT: Human DNA ligases are enzymes that are indispensable for DNA replication and repair processes. Among the three human ligases, ligase I is attributed to the ligation of thousands of Okazaki fragments that are formed during lagging strand synthesis during DNA replication. Blocking ligation therefore can lead to the accumulation of thousands of single strands and subsequently double strand breaks in the DNA, which is lethal for the cells. The reports of the high expression level of ligase I protein in several cancer cells (versus the low ligase expression level and the low rate of division of most normal cells in the adult body) support the belief that ligase I inhibitors can target cancer cells specifically with minimum side effects to normal cells. Recent publications showing exciting data for a ligase IV inhibitor exhibiting antitumor activity in mouse models also strengthens the argument for ligases as valid antitumor targets. Keeping this in view, we performed a pharmacophore-based screening for potential ligase inhibitors in the Maybridge small molecule library and procured some of the top-ranking compounds for enzyme-based and cell-based *in vitro* screening. We report here the identification of novel ligase I inhibitors with potential anticancer activity against a colon cancer cell line.
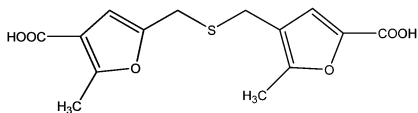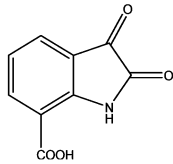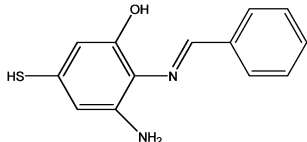
1. INTRODUCTION

DNA ligases are enzymes that join DNA molecules together. They do so by joining adjacent 3′-hydroxyl and 5′-phosphoryl termini to form a phosphodiester bond in duplex DNA. They were first reported by the Gellert, Lehman, Richardson, and Hurwitz laboratories in 1967.[1] Inhibiting the function of ligases can have potentially serious consequences for DNA replication and repair events, processes that are most often targeted in cancer therapy.[2−4] DNA ligases are grouped into two families of ATP-dependent and NAD+-dependent ligases, according to the cofactor required for ligase–adenylate formation.[1,5,6] Human ligases fall into the ATP-dependent family of ligases. The reaction mechanism for ATP-dependent ligases involves the formation of a covalent enzyme-AMP intermediate from the cleavage of ATP to AMP and pyrophosphate. The adenylate group from AMP is then transferred to the 5′-phosphate of the nicked DNA molecule. Finally, the DNA ligase seals the gap by phosphodiester bond formation, via the displacement of the AMP residue with the 3′-hydroxyl group from the adjacent DNA strand.[7,8]

There are three known human DNA ligases (hLigI, III, and IV) performing some vital functions in the body.[9−12] Among them, DNA ligase I has an indispensable role in replication. During replication, the two antiparallel strands of DNA are copied differently. One strand is copied in a continuous manner (and called the leading strand), whereas the other strand, due to its opposite orientation, is copied discontinuously in small stretches called Okazaki fragments, after its discoverer Reiji Okazaki. These fragments then have to be sealed together to make a continuous strand of DNA called the lagging strand. This important function during replication is performed by DNA ligase I. It is also involved in other important DNA repair processes such as nucleotide excision repair (NER)[13,14] and Base excision repair (BER)[15−17] and microhomology-mediated end-joining (MHEJ).[18] The hLigIII is involved in the backup function of Okazaki fragment joining as well as in NER, BER, and MHEJ.[14−19] The hLigIV enzyme is mostly restricted to

Table 1. Structure of Three Compounds[28] and Their IC$_{50}$ Values Used in Generation of the Pharmacophore Model

S.No	Structure	IC$_{50}$ (μM)
1	 Compound: 197	0.6±0.5
2	 Compound: 25	4±2
3	 Compound: 189	5±2

double strand break repair pathways like nonhomologous end-joining (NHEJ).[20,21] Consequently, severe cell lethality, increased genomic instability, and hypersensitivity to DNA damage can be caused by deficiency in DNA ligation. Tomkinson et al. has mentioned that an individual with an inherited mutation in the hLigI gene exhibited retarded growth and development and immunodeficiency.[12] Microcephaly and immunodeficiency are associated with DNA ligaseIV deficiency (LIG4 syndrome) and severe combined immunodeficiency with microcephaly, growth retardation, and sensitivity to ionizing radiation due to NHEJ1 deficiency (NHEJ1 syndrome).[22] No patients with ligase III deficiency have been identified to date.

The levels of hLigI have been found to be high in several cancers compared to normal cells,[23−25] and hence, there is a high probability that hLigI may serve as a good target for cancer therapy. Accumulation of single strand breaks followed by double strand breaks in subsequent cycles of replication is the hallmark of cells deficient in hLigI protein. Several inhibitors against hLigI have been reported, but there is a need for the development of more potent specific inhibitors that can be used in therapy.

During the past few years, virtual screening (VS) has become a potent and established tool for identification of novel hits. The identification of compounds having a desired activity that structurally depart from known active reference compounds and represent new chemotypes is the primary goal of VS.[26] This includes both ligand-based screening approaches, through which test compounds structurally unrelated or a set of known active compounds can be identified, and structure-based virtual screening methods, through which molecules that complement the target protein active site can be identified.[27]

In the present study, we have employed a pharmacophore-based virtual screening approach for searching novel hLigI inhibitors within a commercially available Maybridge database containing more than 56,000 compounds. On the basis of previously reported inhibitors of the targeted protein, a pharmacophore model was generated. The hit molecules identified through the pharmacophore-based virtual screening

were subjected to docking into the protein active site. Further, their electrostatic binding free energy was calculated, and the short-listed compounds were subjected to biological assay.

2. MATERIALS AND METHODS

In the sections below, we report the pharmacophore modeling and *in silico* screening of the Maybridge compound library for human DNA ligase inhibitors and report the identification of a new DNA ligase inhibitors that show specific anticancer activity in colon cancer cell line.

2.1. Generation of Pharmacophore Models and Selection of Data Set. For generation of the pharmacophore model, the top three inhibitors of hLigI were selected from the work of Tomkinson et al.[28] All compounds were drawn by using a sketch module of the molecular modeling suite Sybyl 7.1.[29] The geometries of these compounds were then optimized by Sybyl 7.1 using the Tripos force field and Gasteiger−Huckel charges.[30] The energy minimization was done using the Powell method with an energy convergence gradient of 0.001 kcal mol^{-1}. A set of pharmacophore models was generated using the GASP module of Sybyl 7.1.[31] GASP uses a genetic algorithm (GA) for the superimposition of sets of flexible molecules. GA is used for determining the association between functional groups in the superimposed molecules and the alignment of these groups in the common geometry for receptor binding. In GA, the molecules are treated as a chromosome that trains about flexible bonds and mapping between a hydrogen bond donor proton, acceptor lone pair, and ring center features in pairs of molecules. The fitness function employed in GA is actually a weighted combination of the number and similarity of features that have been aligned, the volume integral of the overlaid molecules, and the van der Waals energy of the conformation of molecules defined by the torsional angles encoded in the chromosomes.[32]

Table 1 shows the structure and IC$_{50}$ values of three inhibitors that have been used for the generation of pharmacophores used in this study. A UNITY query was prepared by mining the chemical features and applying the distance constraints of the GASP-generated pharmacophore

model. The query was consequently modified to optimize both selectivity and specificity. The subset of World of Molecular Bioactivity (WOMBAT) database is considered here as decoy or inactive set,[33] and a set of known inhibitors was put in the test data set[34−40] considered as the active set for the validation of the pharmacophore model.

2.2. Pharmacophore Validation. Validation of the pharmacophore model was performed with the aim to verify its ability to discriminate between active molecules and inactive molecules in the database. The quality of the pharmacophore model was validated using the test set and decoy set methods. Various statistical parameters such as percentage yield of actives, percent ratio of actives, enrichment factor (EF), false negatives, false positives, and goodness of hit score (GH) were further calculated.[41]

2.2.1. Test Set. The test set is used to check whether the generated pharmacophore model is able to retrieve active compounds. The geometry of the entire test set molecules was generated in the same manner as that for the compounds used in pharmacophore model generation.

2.2.2. Decoy Set. The WOMBAT database as the decoy set is used to analyze the discriminating power of the best model by calculating the goodness of hit score (GH) and enrichment factor (EF).

In particular, for determining the discriminatory power of pharmacophore models, a goodness of hit list (GH) is calculated as follows[42]

$$GH = \left[\frac{(H_a)}{4H_tA}(3A + H_t) \times \left(1 - \left(\frac{H_t - H_a}{D - A} \right) \right) \right]$$

where H_a is the number of active hit molecules screened, H_t is the number of total hit molecules screened, A is the number of active molecules in the database, and D is the total number of molecules in the database.

The enrichment factor (EF) shows how many times more active molecules are identified by the model than by a random selection of the same number of compounds, and it is given by the following[42]

$$EF = (H_a \times D)/(H_t \times A)$$

2.3. Database Searching and Ranking of Hit Molecules. The validated pharmacophore model was used as a three-dimensional (3D) structural query for retrieving compounds from the Maybridge database using the UNITY module incorporated with Sybyl 7.1.[43] UNITY is a database screening and scrutinizing tool that is proficient to perform 2D and 3D as well as flexible searches. By default, UNITY 3D database screening performs a prefiltering of database compounds discarding all molecules that do not match Lipinski's rule of five.[44] The compounds identified by the search were further ranked according to the UNITY score.

2.4. Target Structure Preparation and Molecular Docking. The crystal structure of hLigI was retrieved from the Protein Data Bank (PDB ID: 1X9N),[45] and this structure is a complex with co-crystallized deoxyribonucleotide moieties. The deoxyribonucleotides were removed from the complex. Hydrogen atoms were then added followed by energy minimization using Sybyl 7.1 with default values. The resulting structure was then used for docking of hit molecules identified by virtual screening performed on a Silicon Graphics Origin300 server running under an IRIX6.5 operating system with the use of the FlexX module of Sybyl 7.1. The docking method

implemented in FlexX is based on an incremental construction algorithm that first splits the compound into its basic fragments and automatically selects the base fragment by the use of a pattern recognition technique called pose clustering and positions it into an active site followed by the incremental building of the remaining portion onto the active site. The conformational flexibility of the ligand is included by generating multiple conformations for each fragment, and placement of the ligand is scored to estimate the free energy of binding of protein−ligand interactions.[46]

2.5. Electrostatic Binding Free Energy Calculation and Rescoring of Top Hits. The Adaptive Poisson−Boltzmann Solver (APBS) software was used for computing the electrostatic contribution of the binding free energy of the ligand and protein complex.[47] It helped to select the final ranked set of top hits. It works with the combination of molecular mechanics with continuum solvation models. The ligand conformations obtained after the docking process with hLigI were used as an input for binding energy calculations. The PDB format of hLigI and the ligands complex was converted to a PQR format by using the PDB2PQR program.[48] AMBER force field parameters were assigned to the hLigI protein structure.

The method employed in the calculating binding free energy describes the mechanism of the binding process into two components: (1) desolvating the opposing surfaces of both ligand and receptor and then (2) allowing the charges of the two molecules to interact. It is then possible to disentangle the change in electrostatic free energy on molecular association (ΔG_{ele}^{bind}) into three components: (1) the change in electrostatic desolvation free energies of the ligand upon binding (ΔG_{desol}^{L}), (2) the change in electrostatic desolvation free energies of the receptor upon binding (ΔG_{desol}^{R}), and (3) the ligand receptor interaction energy in the presence of the surrounding solvent (ΔG_{ele}^{LR}). The electrostatic binding free energy (ΔG_{ele}^{bind}) is defined as the following[49,50]

$$\Delta G_{ele}^{bind} = \Delta G_{desol}^{L} + \Delta G_{desol}^{R} + E_{ele}^{LR}$$

The loss of electrostatic interaction between the solvent and receptor (or ligand) upon binding is characterized the electrostatic contribution to the desolvation energy of the receptor (ΔG_{desol}^{R}) and is calculated in the two-step method used by Perez et al.[51]

2.6. *In Vitro* DNA Ligation Assay. DNA ligation assay was done essentially as described by Chen et al.[52] Three different single strand DNA oligos, 52-mer (5′-GTACGTCGATC-GATTGGTAGATCAGTGTCTATGTATGTCAGTGAGA-TAGTAC-3′), 25-mer (5′-CTGATCTACCAATCGATC-GACGTAC-3′) and 27-mer (5′-/5Cy3/GTACTATCTCACT-GACATACATAGACA-3′) were annealed to form a double-stranded nicked substrate for the ligase enzymes. The 27-mer oligo was labeled at the 5′ end with a fluorescent dye cyanin3 (Cy3) for easy detection on the GE Life Sciences LAS4010 detector. The reaction mixture (20 μL) contained 1 pmol of labeled DNA substrate and 0.2 pmol of purified hLigI in a ligation buffer containing Tris-Cl (50 mM, pH 7.5), MgCl$_2$ (10 mM), BSA (0.25 mg/mL), NaCl (100 mM), and ATP (500 μM). The double-stranded nicked DNA was incubated with the purified ligase in the absence or presence of inhibitors at 37 °C for 30 min. Reactions were stopped by adding 10 μL of stop buffer (90% formamide and 10% of 50 mM EDTA). The ligated DNA molecule would be larger in size and run higher up in denaturing gel containing 7 M urea and 12% acrylamide. If an inhibitor is added to the reaction mixture, this would lead to

an inhibition of ligation and a corresponding loss of labeled ligated product in the gel. We would then be able to calculate the percentage of inhibition of ligation by estimating the density (by image quant LAS 4010) of ligated product in the lane without inhibitor and comparing it with the lanes containing different inhibitor molecules or with the same inhibitor molecule at different concentrations.

2.7. Electrophoretic Mobility Shift Assay (EMSA). EMSA was performed with a double stranded, fluorescein dye (FAM) labeled oligo as substrate for ligase I protein. Of the three oligos used to make the substrate, one was a 5′-FAM labeled 27-mer oligo with a dideoxy modified 3′ end (5′-/56-FAM/GTACTATCTCACTGACATACATAGAC/3ddc/−3′). Other two oligos are 25-mer(5′-CTGATCTA-CCAATCGATCGACGTAC-3′) and 52-mer (5′-GTACGT-CGATCGATTGGTAGATCAGGGTCTATGTATGTCA-GTGAGATAGTAC-3′). These oligos were annealed to obtain a non-ligatable nicked substrate for the ligase I protein. We incubated 10 pmole of hLigI with 50, 100, and 200 μM inhibitors and 2 pmole non-ligatable single-nicked substrate DNA in a ligation buffer containing Tris-Cl (50 mM, pH 7.5), MgCl$_2$ (10 mM), BSA (0.25 mg/mL), NaCl (100 mM), and ATP (500 μM) in a reaction volume of 20 μL for 2 h on ice. After the addition of 10 μL of native gel buffer (tris (pH 7.5) 50 mM, 20% glycerol, 0.05% bromophenol blue), samples were separated by 6.5% native PAGE, and bands were detected by image quant LAS4010.

2.8. DNA Intercalation Assay. To determine whether the ligation inhibition occurs due to DNA intercalation, we performed the DNA intercalation assay. In this case, we incubated 100 ng of linearized pUC18 plasmid with increasing concentrations (50, 100, 200 μM) of the inhibitors for 30 min at 37 °C before running the mixture in an agarose gel. Doxorubicin (positive control) and ampicillin (negative control) were used as controls for DNA intercalation. Reaction products were resolved on a 1% agarose gel at 5.3 V/cm. Gel was visualized by ethidium bromide staining.

2.9. SRB Assay. Various cancer cell lines were obtained from the American Type Culture Collection (ATCC), U.S.A. These cells were grown in recommended media supplemented with 10% FBS and PenStrep in a 5% CO$_2$-humidified atmosphere at 37 °C. No cultures beyond 25 passages were used for the study. A standard colorimetric SRB (sulforhod-amine B) assay was used for the measurement of cell cytotoxicity. In brief, 5000 cells were added to each well of a 96-well plate and treated with 10/100 μM of test compounds, and untreated cells received the same volume of DMSO as a vehicle control. After 48 h of exposure, cells were fixed with ice-cold TCA, stained with SRB in 1% acetic acid, and washed. Bound dye was dissolved in a 10 mM Tris base, and absorbance values were measured at 510 nm on a plate reader (Epoch Microplate Reader, Biotek, U.S.A.). The cytotoxic effects of compounds were calculated as % inhibition in cell growth as per the formula [100 − (absorbance of compound treated cells/absorbance of untreated cells)] × 100.

2.10. Determination of IC$_{50}$ Values. IC$_{50}$ was determined by incubating the cells in five incremental concentrations of the inhibitor from 2 to 10 μM concentrations. For this purpose, 5000 cells of DLD-1 were plated onto 96-well plates and let to adhere for 12 h. After 12 h, inhibitors were added and incubated for 48 h. The SRB assay was then performed, and the concentration of the inhibitor that inhibited 50% cellular

growth of cells was determined using the Prism Graphpad software.

3. RESULTS AND DISCUSSION

3.1. Pharmacophore Generation. The overall computational process employed in the study is shown in Figure 1. A set
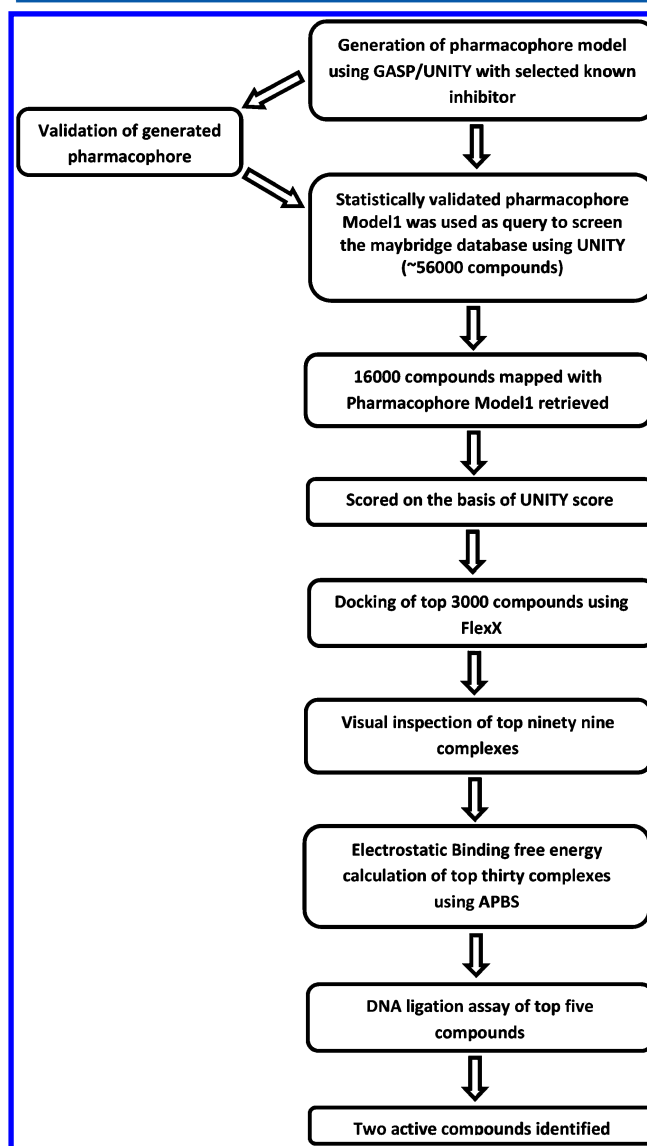

Figure 1. Flowchart showing the methodology applied in the present study.

of four pharmacophore models was generated using GASP with the help of selected inhibitors. The four models generated are shown in Figure 2. Various statistical parameters were calculated for these models and are discussed in the next section. Model 4 did not identify any molecule from the test set or decoy set; hence, it was not considered for statistical evaluation. The pharmacophore models included in the statistical evaluation consist of three features generated by GASP alignment: one hydrophobic feature and two acceptor atoms.

3.2. Pharmacophore Validation. A good pharmacophore model should be able to enrich the maximum biologically active molecules from a structurally diverse data set as well as to reject
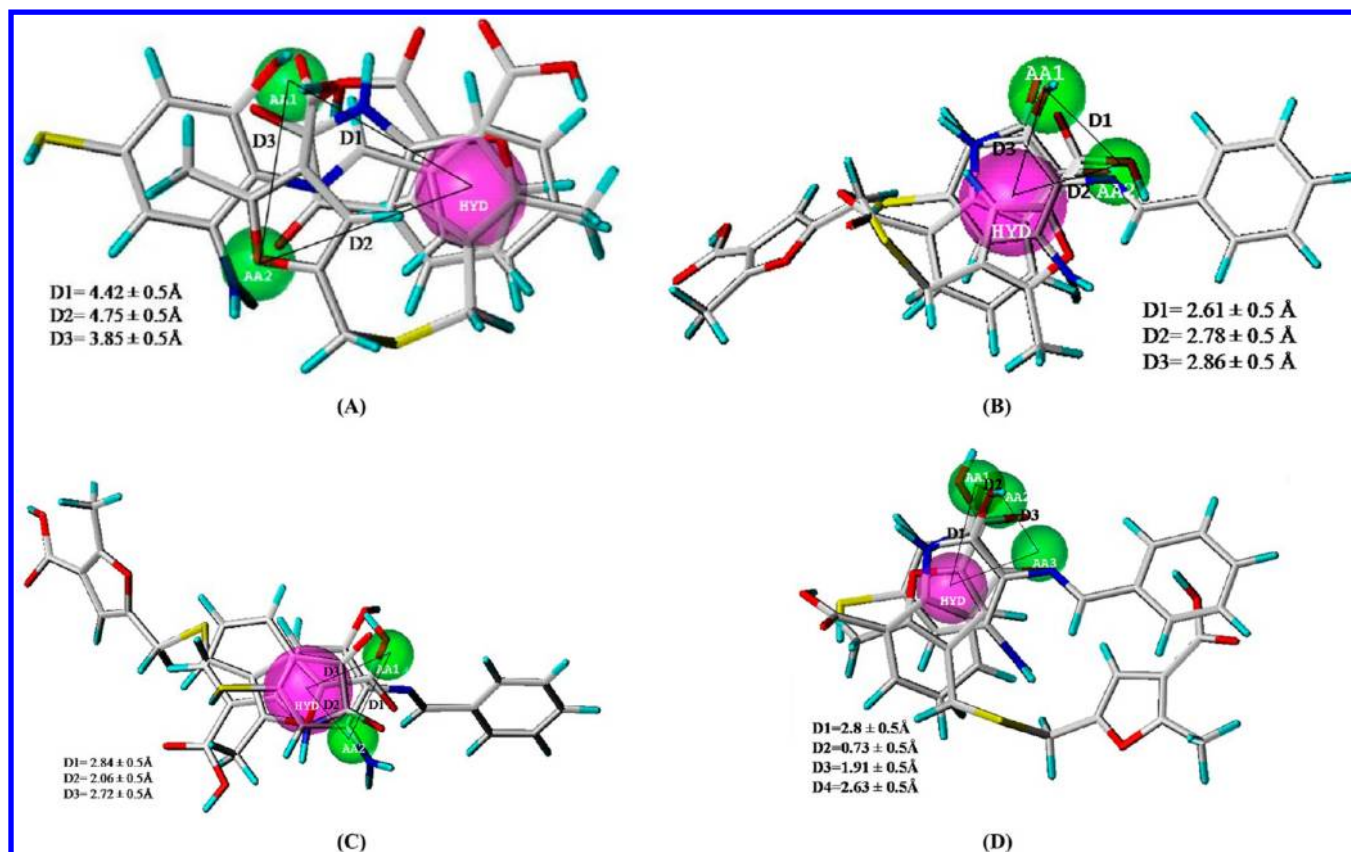
Figure 2. Pharmacophore models generated with GASP. (A) Best validated pharmacophore model 1 containing acceptor atoms (AA1 and AA2) and one hydrophobic group (HYD). D1, D2, and D3 are distance among these features. Sphere sizes indicate query tolerances. (B) Model 2. (C) Model 3. (D) Model 4.

most of inactive molecules. To validate the consistency of the pharmacophore models, they were subjected to screening the test set containing 33 compounds and a subset of WOMBAT consisting of 1204 molecules, which are considered here as inactive for hLigI because they are active against other proteins.

The enrichment factor (EF), goodness of hit (GH), and other statistical values have been calculated for the three selected pharmacophore models using the test set and WOMBAT database. Model 1 showed an EF value of 24.50 by mapping 17 active compounds from the 26 screened compounds from the database. The EF values for model 2 and model 3 were 9.37 and 5.26 as they retrieved 13 and 8 active compounds, respectively. The higher is the EF value, the greater is the ability of a pharmacophore in identifying the active compounds. Model 1 has a GH value of 0.614, while model 2 and model 3 have GH values of 0.277 and 0.160, respectively. This validation result, which is tabulated in Table 2, shows that model 1 (Figure 2A) with a minimum false positive and false negative and good EF value and GH score was capable enough to be used in the further screening of the Maybridge database to identify novel leads. Model 1 was selected for further study, and although it is very simple and has only three pharmacophoric features, it has been statistically validated. In the past, there have been studies reported in the literature where three-point pharmacophore models were generated and used for the identification of novel lead molecules against several protein targets.[53,54]

3.3. Database Searching and Scoring. Database searching was performed using UNITY with model 1. In the UNITY search, the compounds present in the database are

Table 2. Statistical Parameters Obtained After the Screening of Test Set Molecules for the Pharmacophore Model

parameter	model 1	model 2	model 3
total no. of molecules in database (D)	1237	1237	1237
total no. of actives in database (A)	33	33	33
total hits (H_t)	26	52	57
active hits (H_a)	17	13	8
% yield of actives ($H_a/H_t \times 100$)	65.38%	25.00%	14.03%
% ratio of actives ($H_a/A \times 100$)	51.51%	39.39%	24.24%
enrichment factor (EF)	24.50	9.37	5.26
false negative ($A - H_a$)	16	20	25
false positive ($H_t - H_a$)	9	39	49
goodness of hit score (GH)	0.614	0.277	0.160

subjected to a conformational flexible 3D alignment based on the direct tweak's algorithm. In this algorithm, low energy conformers are generated for each compound in the database that possesses the shortest distance to the model features. Thus, there is no need of a conformational model for database compounds, and the VS is hastened by evading fitting of a large number of compound conformers. The partial matching of pharmacophore features is also allowed in UNITY.[55]

As a result of a flexible search, we found 16,000 hits out of 56,000 molecules that were mapped to the pharmacophore model. Figure 3A and B shows the active compounds mapped on pharmacophore model 1. The compounds identified by the search were further ranked according to the UNITY score. The ranking of the hit list was done using the simple scoring function implemented in UNITY, where R_{energy}, R_{bond}, and R_{rms}
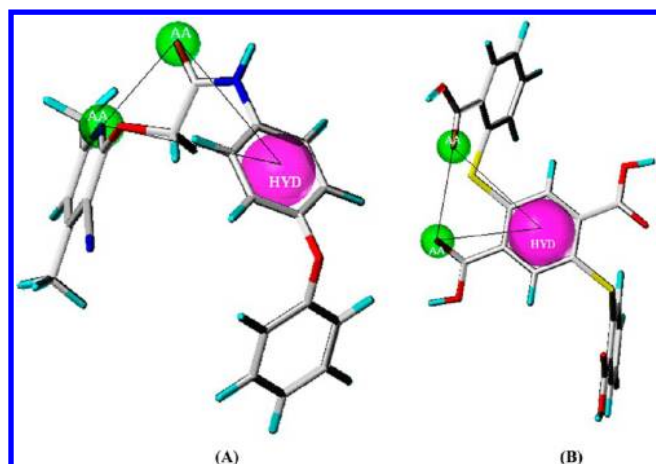
Figure 3. Selected active compounds (A) HTS01682 and (B) NRB00556 aligned on pharmacophore model 1.

are the ranks of the hits by energy, number of rotatable bonds, and RMS, respectively. The smaller the score is, the better the hit is. The score is calculated from the following[56]
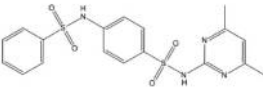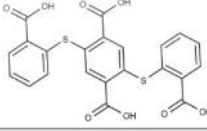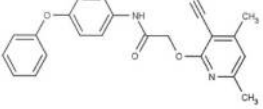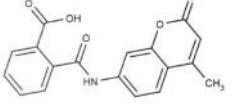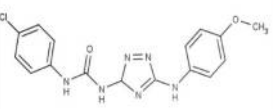
$$Score = R_{energy}\sqrt{R_{bond} + R_{rms}}$$

3.4. Molecular Docking. A putative DNA binding site within the DBD was identified in the crystal structure of hLigI (PDB ID: 1X9N), which is co-crystallized with DNA. For the docking procedure, we focused on four residues, His337, Arg449, Arg451, and Gly453 that are located in the central

region of the DBD and make direct contacts with the DNA substrate.[24] This region was inspected meticulously to identify the residues that are involved in DNA binding, and then those residues were selected for the active site, which are engaged in making a hydrogen bond with DNA. Initially, we docked the three inhibitors[28] to this active site to optimize the parameters of the docking program and also to validate our selected active site. All these inhibitors docked well at this site. The top 3000 compounds obtained by scoring of the identified hits were subjected to docking into the above-mentioned active site. The binding modes were generated according to the FlexX scoring scheme (Table 3), which is represented by the structure with the most favorable binding free energy (ΔG_{bind}). The top-scoring docked conformations of 99 compounds, having energy greater than −25.00 kcal/mol, in the active site of hLigI were retrieved and analyzed in terms of the favored mode of binding of the molecules and key residues employed in the interaction.

3.5. Binding Energy Analysis. An imperative constraint for a successful VS experiment is to precisely predict the binding energies of the docked conformation. In this perspective, our VS protocol applied the use of the binding free energy calculation to propose the final ranked set of top 30 hits. Presently, it has been validated as a VS refining tool to prioritize active hits.[57] Table 3 shows the APBS binding free energy to that of FlexX for the top five complexes selected for biological assay. There are differences in the binding energy of FlexX and APBS; this is because FlexX does not calculate the columbic contribution from all of the atoms in the protein like APBS. As our initial goal was to identify compounds with better

Table 3. Docking Energy, Electrostatic Binding Energy (BE), and Ligase Inhibition Activity of Five Compounds Subjected to Ligation Assay

S.No	Name	Structure	Electrostatic BE(kcal/mol)	Docking energy by FlexX (kJ/mol)	Inhibition of ligase activity (IC$_{50}$)
1	HTS07250		−28.9307	−28.444	>100μM
2	NRB00556		−28.0327	−37.363	37.56±6.97μM
3	HTS01682		−25.6239	−28.548	24.93±3.71 μM
4	HTS07014		−17.9523	−28.897	>100μM
5	TG00130		−16.4692	−28.897	>100μM

binding affinity, in the course of this, we have reranked our top 30 docked complexes to achieve the final set of proposed hits based on their electrostatic binding free energy. The binding energy of the top 30 docked complexes is given in Table 1 of the Supporting Information.

The five compounds were purchased among the top 30 compounds after analyzing their binding energy as predicted by FlexX and APBS and also the mode of interaction as predicted by docking simulations. The compounds HTS07250, NRB00556, HTS01682, HTS07014, and TG00130 were purchased as per their availability and subjected to DNA ligation assay, and we have found that HTS01682 and NRB00556 significantly inhibit the ligation process accomplished by hLigI. The binding energy was found to be −28.0327 and −25.6239 kcal/mol for the active compounds NRB00556 and compound HTS01682, respectively.

3.6. In Vitro Screening of Putative hLigI inhibitor. Out of the 30 compounds selected from in silico screening, five compounds were tested compounds (HTS01682, HTS07250, HTS07014, NRB00556, and TG00130) in our in vitro studies. We first performed fluorescent-based ligation assays at 100 μM concentration for hLigI (Figure 4). HTS01682 demonstrated the maximum inhibition of ligation of 91.22 ± 4.18%, while NRB00556 with 86.5 ± 4.82% inhibition and TG00130 with 56.75 ± 8.51% inhibition, respectively, (lanes 3, 6, and 7) also showed significant inhibition of ligation. The compounds HTS07250 and HTS07014, however, did not inhibit hLigI
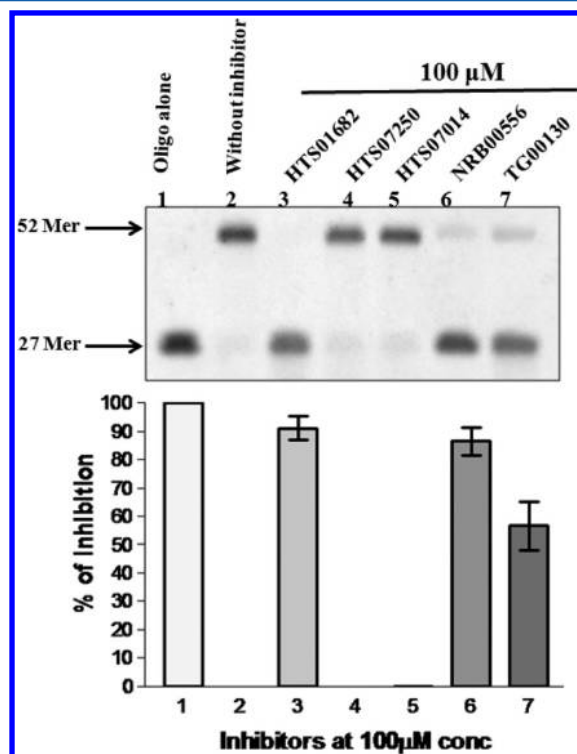

Figure 4. Inhibition of DNA ligase I activity for compounds HTS01682, HTS07250, TG00130, NRB00556, and HTS07014 at 100 μM concentrations. HTS01682 showed maximum inhibition of ligation of about 91.22 ± 4.18%, while NRB00556 showed 86.5 ± 4.82% inhibition and TG00130 showed 56.75 ± 8.51% inhibition of ligase I activity, respectively (lanes 3, 6, and 7). HTS07250 and HTS07014 did not inhibit hLigI significantly (lanes 4 and 5). Lane 1 was a control with no ligase, and lane 2 contained only the ligase I protein but no inhibitor.

significantly (lanes 4 and 5). Lane 1 was a control with no ligase, and lane 2 contained only the hLigI and DMSO but no inhibitor.

3.7. Specificity and Kinetics of Ligase Inhibitors. We performed a concentration-dependent ligation inhibition assay for the active compounds against various human and non-human DNA ligase proteins such as hLigI, hLigIIIβ, hLigIV/XRCC4, and T4 DNA ligase. We also checked whether the inhibitors exhibited concentration-dependent (25, 50, 100 μM) ligation inhibition activity. The active compounds (HTS01682 and NRB00556) were tested as shown in Figure 5. We observed that these compounds demonstrated dose-dependent ligation inhibition activity against hLigI with 50% ligation inhibition at 24.93 ± 3.71 μM for HTS01682 and 37.56 ± 6.97 μM for NRB00556. Although the compounds have some overlapping activity against hLigIIIβ, they are completely inactive against hLigIV/XRCC4 and T4 DNA ligases. Hence, these compounds specifically inhibit the activity of hLigI with some overlapping activity against hLigIIIβ.

3.8. Mechanism of Inhibition of Ligase Inhibitors. There are several modes by which a compound can inhibit ligation.[4] Two of the most common modes are by direct interaction with the ligase protein (hence, occluding the binding of ligase from the substrate DNA) or by intercalation with DNA, thereby restricting the access of DNA from the ligase. To check direct binding, we performed Electrophoretic Mobility Shift Assays (EMSA). This experiment works on the principle that the ligase enzyme binds to DNA and forms a complex that runs higher up on a gel than the DNA when run alone (Figure 6A and B, lane 1 versus lane 2). Now if an inhibitor binds, it can do so at either the DNA binding domain of the ligase protein (hence, occluding its binding with DNA) or bind to an allosteric site, in which case it may form a bigger ligase−DNA−inhibitor complex. As shown in Figure 6 A, HTS01682 reduces the hLigI-nicked DNA complex at higher concentrations (lanes 3−5). Such a reduction in a hLigI−DNA complex can occur only due to competition between inhibitor and substrate DNA for binding with DBD of the ligase protein. In contrast, in Figure 6 B, at increasing concentrations (lanes 3−5), NRB00556 stabilizes and increases the hLigI-nicked DNA complex. The explanation in this case is that NRB00556 stabilizes the ligase−DNA complex so that the ligase cannot complete the ligation step, although it maybe able to bind the DNA.

To rule out other modes of inhibitions of ligation by these inhibitors, we also checked the DNA intercalation property of these inhibitors. This experiment works on the principle that any molecule that intercalates with DNA will pose a hindrance to the movement of DNA in an agarose gel, as compared to when there is no intercalator in the DNA. In Figure 7, unlike the known DNA intercalator doxorubicin, there was no hindrance shown in the movement of DNA in the presence (even at 200 μM concentration) of hLigI inhibitors. Hence, we can infer from these experiments that the inhibition of ligation shown by the active compounds is through a direct interaction between the compound and the protein (HTS01682) or protein−DNA complex (NRB00556) and not through DNA intercalation.

To explore the mechanism of inhibition in more detail, the binding modes of the two most active compounds were analyzed comprehensively. Figure 8A demonstrates the binding modes obtained from docking of the two biologically active molecules in the DNA binding region of the catalytic site of
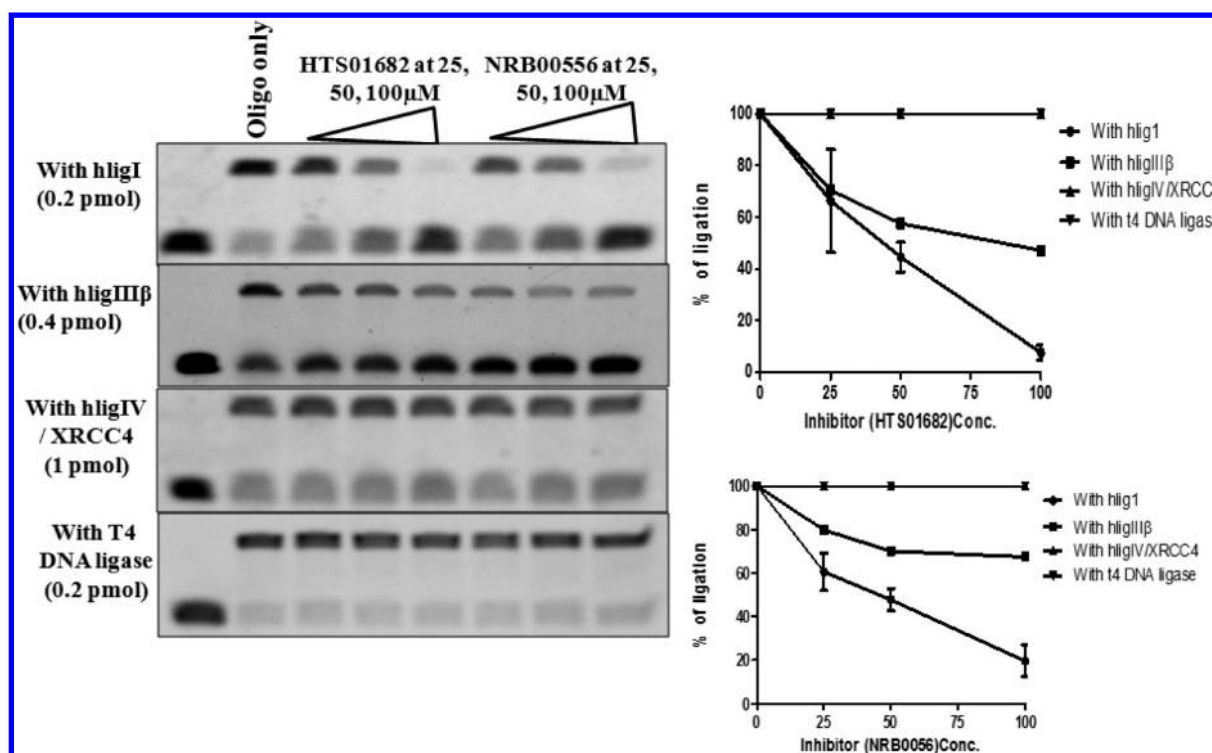
G

dx.doi.org/10.1021/ci5000032 | J. Chem. Inf. Model. XXXX, XXX, XXX−XXX

Figure 5. Concentration-dependent ligation inhibition activity for the active compounds HTS01682 and NRB00556 at 25, 50, and 100 μM concentrations against various ligase proteins. Top left panel clearly demonstrates that both compounds are specific inhibitors of human ligase I protein. No significant inhibition was observed for the activity of hLigIIIβ (left panel, second from top), hLigIV/XRCC4 (left panel, third from top), or T4 DNA ligase protein (left panel, bottom). The graphs on the right also clearly show that both inhibitors inhibit human ligase IIIβ activity by 50% and 30%, respectively.
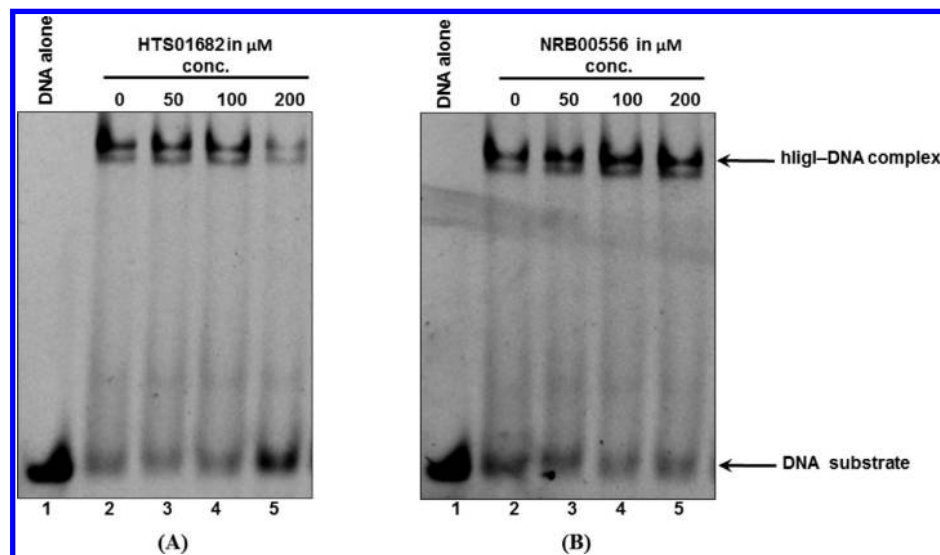

Figure 6. Electrophoretic mobility shift assay (EMSA) was performed with the active ligase inhibitors HST01682 and NRB00556 at 50, 100, and 200 μM concentrations. In panel A, the compound HTS01682 reduced the hLigI-nicked DNA complex at higher concentrations (lanes 3−5), whereas in panel B, the compound NRB00556 stabilizes the hLigI-nicked DNA complex at higher concentrations (lanes 3−5). This suggests different modes of inhibition for the two compounds.

ligase I and formation of the hydrogen bond with DNA binding residues including Arg451, Gly453, Lys768, and Lys770. The overall pattern of binding was found to be similar for these compounds. A visual inspection of the docked complexes shows that the selected molecules are accommodated fairly well in the binding pocket and occupied the same position. Figure 8B shows the binding mode of HTS01682. A thorough inspection

of the complex was done in order to identify those interactions that might play an important role in binding DNA to protein and in turn may be important for ligation. By preventing contact of DNA from these residues, the ligation process may be inhibited. The binding mode of compound HTS01682 was analyzed in terms of residues of hLigI that are involved in the interaction with DNA. Side chain nitrogen of Arg449 forms two
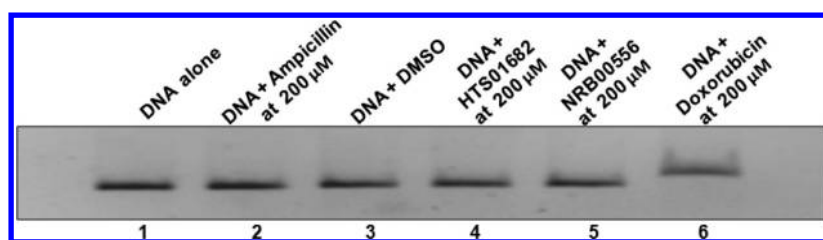
H

dx.doi.org/10.1021/ci5000032 | J. Chem. Inf. Model. XXXX, XXX, XXX−XXX

Figure 7. DNA intercalation assay was performed for the compounds HTS01682 and NRB00556. No change in migration of the DNA was observed on a 1% agarose gel as compared with the negative control ampicillin (lane 2), vehicle control DMSO (lane 3), or DNA alone (lane 1). However, the addition of the known DNA intercalator doxorubicin to the same DNA led to a hindrance in migration as shown by the higher migrating band in lane 6 (positive control).
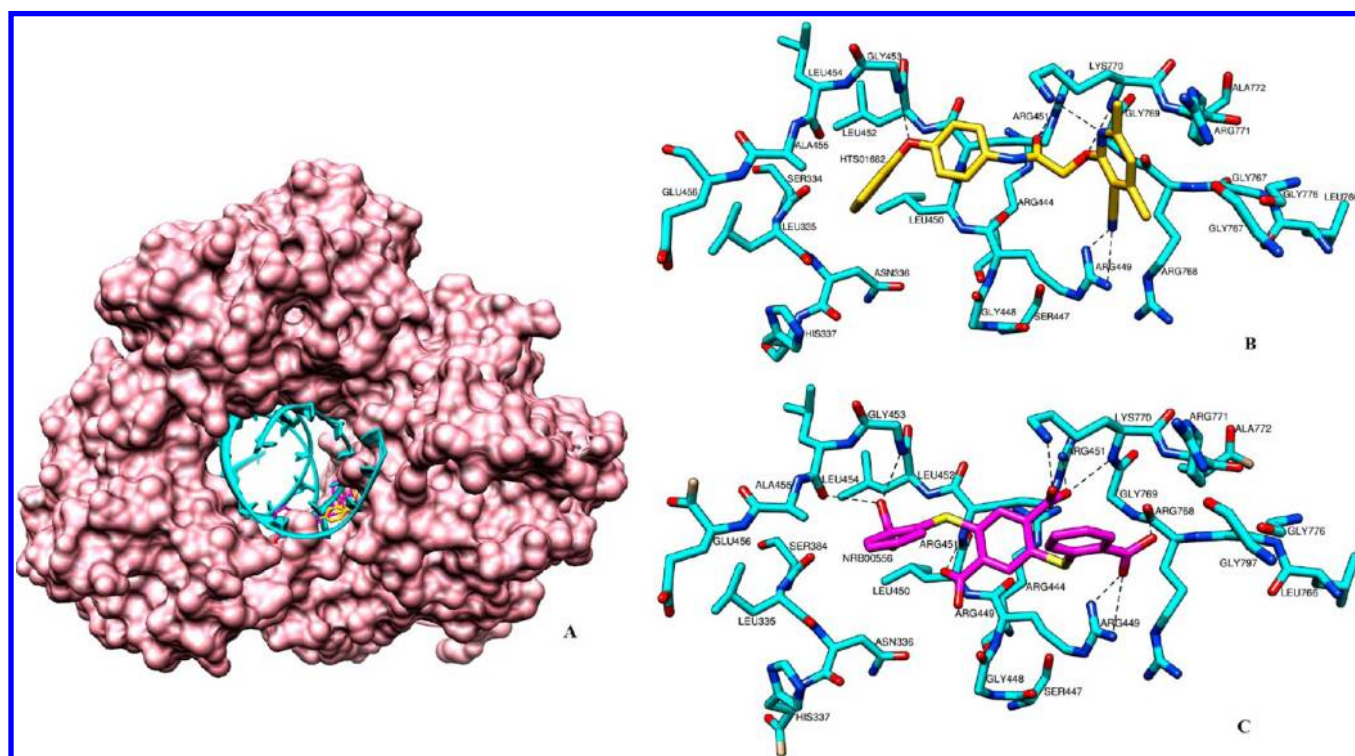

Figure 8. (A) Two active compounds HTS01682 (yellow) and NRB00556 (pink) in the hLigI. DNA is shown as cyan ribbon, and the molecules occupy the location where DNA is present in the crystal structure. Docking of selected compounds in the DNA binding site of hLigI is shown in panels B (HTS01682) and C (NRB00556). Hydrogen bonds are black dashed lines. Protein residues are cyan in color.

Table 4. Antiproliferative Activity of Ligase Inhibitors HTS01682 and NRB00556 Tested by a SRB Assay at 10 μM Concentration against an Array of Cancer Cell Lines[a]

compounds at 10 μM conc.	% inhibition in prostate cancer (PC3)	% inhibition in renal cancer (786-O)	% inhibition in colon cancer (DLD-1)	% inhibition in colon cancer (SW-620)	% inhibition in brain cancer (A172)	% inhibition in breast cancer (MCF-7)	% inhibition in lung cancer (A549)	% inhibition in liver cancer (PLC/PRF/5)	% inhibition in normal fibroblast (NIH/3T3)
HTS01682	40.8	26.5	75.4	19.7	−14.3	5.6	14.9	21.5	15.24
NRB00556	10.0	8.7	57.6	5.1	−1.7	−2.6	1.8	17.2	3.19

[a]Both compounds showed maximum antiproliferative activity against the colon cancer cell line DLD-1. The HTS01682 molecule clearly showed greater antiproliferative activity of 75.4% as opposed to 57.6% antiproliferative activity for NRB00556 at 10 μM concentration. The HTS01682 molecule also showed an appreciable antiproliferative activity of 40.8% against the prostate cancer cell line PC3. No antiproliferative activity was observed for either compound against any of the other cell lines tested, hence indicating its selective nature.

hydrogen bonds with a CN group attached to a pyrimidine moiety of this molecule. The side chain nitrogen of Arg451 also forms a hydrogen bond with HTS01682. Another important interaction was found between the backbone nitrogen of Gly453 and HTS01682. Side chain nitrogen of Lys770 of hLigI was found to form two hydrogen bonds with the pyrimidine

moiety of HTS01682. All these residues make direct contact with DNA in the crystal structure of hLigI.[45]

Figure 8C shows the binding mode of NRB00556. As shown in the figure, a hydrogen bond forms between the side chain of Arg449 and a carboxyl oxygen attached to one of the benzene rings of NRB00556. The backbone nitrogen of Arg451 also makes two hydrogen bonds with the hydrogens of both of the

I

dx.doi.org/10.1021/ci5000032 | J. Chem. Inf. Model. XXXX, XXX, XXX−XXX

carboxyl groups attached to a second benzene ring of this compound. Lys770 also forms two hydrogen bonds with one carboxyl group attached to the mentioned benzene ring. Gly453 is involved in forming a hydrogen bond with the carboxyl group of another benzene moiety of the compound. Leu454 also forms a hydrogen bond with this carboxyl group. It also interacts with hLigI through hydrogen bonds with Arg768 and Gly448. As discussed earlier, these residues are shown to form hydrogen bonds with DNA in hLigI crystal structures.

3.9. Antiproliferative Activity of Ligase Inhibitors. The effect of the ligase inhibitors HTS01682 and NRB00556 were tested against the growth and proliferation of various cancer cell lines such as PC3, 786-O, DLD-1, PLC/PRF/5, SW620, A172, MCF-7, and A549 by following the NIH-recommended SRB assay at 10 μM concentration. The results from the SRB assay are shown in Table 4. We observed that at the tested 10 μM concentration both compounds demonstrated maximum antiproliferative activity against the DLD-1 (colon cancer) cell line with IC$_{50}$ values of 6.67 and 8.78 μM, respectively. Colon cancer is a dreaded form of cancer affecting a large number of people above 40 years of age. Most colon cancers originate from small noncancerous (benign) tumors called adenomatous polyps that form on the inner walls of the large intestine. Some of these polyps may grow into malignant colon cancers over time if they are not removed during colonoscopies. Colon cancer cells will invade and damage healthy tissue that is near the tumor causing many complications. Once diagnosed with colon cancer, survival depends on what stage of cancer the person is diagnosed with and whether the person responds to available treatment. The present treatment options are often nonspecific or have toxic side effects. The identification of these inhibitors in this study thus has the potential to be developed as a molecularly targeted therapy for the treatment of patients with colon cancer.

4.0. CONCLUSIONS

In this study, pharmacophore modeling and virtual screening led to the identification of novel inhibitors of human DNA ligase I protein. We have applied a multi-step virtual screening protocol including a 3D pharmacophore search, molecular docking, and calculations of binding energy to prioritize the virtual screening hits against hLigI. Some of the top-scoring hits were subjected to ligation assays where two compounds, HTS01682 and NRB00556, inhibited DNA ligation activity significantly in the 25–35 μM range. Hence, our results demonstrate the efficiency of pharmacophore-based virtual screening for the identification of potential hLigI inhibitors that also demonstrate potential anticancer activity against a colon cancer cell line.

■ ASSOCIATED CONTENT

Ⓢ Supporting Information

Information as mentioned in the text. This material is available free of charge via the Internet at http://pubs.acs.org.

■ AUTHOR INFORMATION

Corresponding Authors
*E-mail: mi_siddiqi@cdri.res.in (M.I.S.).
*E-mail: d.banerjee@cdri.res.in (D.B.).

Author Contributions
‖Both authors (S.K. and D.K.S.) contributed equally.

■ REFERENCES

(1) Lehman, I. R. DNA ligase: Structure, mechanism, and function. *Science* **1974**, *186* (4166), 790−797.

(2) Chen, X.; Zhong, S.; Zhu, X.; Dziegielewska, B.; Ellenberger, T.; Wilson, G. M.; MacKerellJr, A. D.; Tomkinson, A. E. Rational design of human DNA ligase inhibitors that target cellular DNA replication and repair. *Cancer Res.* **2008**, *68* (9), 3169−3177.

(3) Srivastava, M.; Nambiar, M.; Sharma, S.; Karki, S. S.; Goldsmith, G.; Hegde, M.; Kumar, S.; Pandey, M.; Singh, R. K.; Ray, P.; Natarajan, R.; Kelkar, M.; De, A.; Choudhary, B.; Raghavan, S. C. An inhibitor of nonhomologous end-joining abrogates double-strand break repair and impedes cancer progression. *Cell* **2012**, *151* (7), 1474−1487.

(4) Singh, D. K.; Krishna, S.; Chandra, S.; Shameem, M.; Deshmukh, A. L.; Banerjee, D. Human DNA ligases: A comprehensive new look for cancer therapy. *Med. Res. Rev.* **2013**, DOI: 10.1002/med.21298.

(5) Wilkinson, A.; Day, J.; Bowater, R. Bacterial DNA ligases. *Mol. Microbiol.* **2001**, *40*, 1241−12481.

(6) Shuman, S. NAD$^+$ specificity of bacterial DNA ligase revealed. *Structure* **2004**, *8*, 1335−1336.

(7) Söderhäll, S.; Lindahl, T. Mammalian deoxyribonucleic acid ligase. Isolation of an active enzyme-adenylate complex. *J. Biol. Chem.* **1973**, *248* (2), 672−675.

(8) Söderhäll, S. Properties of a DNA-adenylate complex formed in the reaction between mammalian DNA ligase I and DNA containing single-strand breaks. *Eur. J. Biochem.* **1975**, *51* (1), 129−36.

(9) Barnes, D. E.; Johnston, L. H.; Kodama, K.; Tomkinson, A. E.; Lasko, D. D.; Lindahl, T. Human DNA ligase I cDNA: Cloning and functional expression in *Saccharomyces cerevisiae*. *Proc. Natl. Acad. Sci.U.S.A.* **1990**, *87* (17), 6679−83.

(10) Wei, Y. F.; Robins, P.; Carter, K.; Caldecott, K.; Pappin, D. J.; Yu, G. L.; Wang, R. P.; Shell, B. K.; Nash, R. A.; Schar, P. Molecular cloning and expression of human cDNAs encoding a novel DNA ligase IV and DNA ligase III, an enzyme active in DNA repair and recombination. *Mol. Cell. Biol.* **1995**, *15* (6), 3206−3216.

(11) Robins, P.; Lindahl, T. DNA ligase IV from HeLa cell nuclei. *J. Biol. Chem.* **1996**, *271* (39), 24257−61.

(12) Ellenberger, T.; Tomkinson, A. E. Eukaryotic DNA ligases: Structural and functional insights. *Annu. Rev. Biochem.* **2008**, *77*, 313−338.

(13) Teo, I. A.; Arlett, C. F.; Harcourt, S. A.; Priestley, A.; Broughton, B. C. Multiple hypersensitivity to mutagens in a cell strain (46BR) derived from a patient with immuno-deficiencies. *Mutat. Res.* **1983**, *107*, 371−386.

(14) Moser, J.; Kool, H.; Giakzidis, I.; Caldecott, K.; Mullenders, L. H.; Fousteri, M. I. Sealing of chromosomal DNA nicks during nucleotide excision repair requires XRCC1 and DNA ligase III alpha in a cell-cycle-specific manner. *Mol. Cell* **2007**, *27* (2), 311−323.

(15) Prasad, R.; Singhal, R. K.; Srivastava, D. K.; Molina, J. T.; Tomkinson, A. E.; Wilson, S. H. Specific interaction of DNA polymerase 13 and DNA ligase I in a multiprotein base excision repair complex from bovine testis. *J. Biol. Chem.* **1996**, *271*, 16000−16007.

(16) Robertson, A. B.; Klungland, A.; Rognes, T.; Leiros, I. DNA repair in mammalian cells: Base excision repair: the long and short of it. *Cell. Mol. Life Sci.* **2009**, *66* (6), 981−993.

(17) Dianov, G. L. Base excision repair targets for cancer therapy. *Am. J. Cancer Res.* **2011**, *1* (7), 845−851.

(18) Liang, L.; Deng, L.; Nguyen, S. C.; Zhao, X.; Maulion, C. D.; Shao, C.; Tischfield, J. A. Human DNA ligases I and III, but not ligase IV, are required for microhomology-mediated end joining of DNA double-strand breaks. *Nucleic Acids Res.* **2008**, *36* (10), 3297−3310.

(19) Kubota, Y.; Nash, R. A.; Klungland, A.; Schar, P.; Barnes, D. E.; Lindahl, T. Reconstitution of DNA base excision-repair with purified human proteins: Interaction between DNA polymerase beta and the XRCC1 protein. *EMBO J.* **1996**, *15*, 6662−6670.

(20) Wilson, T. E.; Grawunder, U.; Lieber, M. R. Yeast DNA ligase IV mediates non-homologous DNA end joining. *Nature* **1997**, *388* (6641), 495−498.

(21) Grawunder, U.; Zimmer, D.; Fugmann, S.; Schwarz, K.; Lieber, M. R. DNA ligase IV is essential for V(D)J recombination and DNA double-strand break repair in human precursor lymphocytes. *Mol. Cell* **1998**, *2* (4), 477−84.

(22) Chrzanowska, K. H.; Gregorek, H.; Dembowska-Baginska, B.; Kalina, M. A.; Digweed, M. Nijmegen breakage syndrome (NBS). *Orphanet J. Rare Dis.* **2012**, *7*, 13.

(23) Teraoka, H.; Sawai, M.; Yamamoto, K.; Tsukada, K. DNA ligase I mRNA and enzyme levels in human hematopoietic cells under dimethyl sulfoxide-induced growth-arrest and differentiation. *Biochem. Int.* **1992**, *26* (5), 963−971.

(24) Jessberger, R.; Schar, P.; Robins, P.; Ferrari, E.; Riwar, B.; Hubscher, U. Regulation of DNA metabolic enzymes upon induction of preB cell development and V(D)J recombination: Up-regulation of DNA polymerase delta. *Nucleic Acids Res.* **1997**, *25* (2), 289−296.

(25) Sun, D.; Urrabaz, R.; Nguyen, M.; Marty, J.; Stringer, S.; Cruz, E.; Medina-Gundrum, L.; Weitman, S. Elevated expression of DNA ligase I in human cancers. *Clin. Cancer Res.* **2001**, *7* (12), 4143−4148.

(26) Bajorath, J. Integration of virtual and high throughput screening. *Nat. Rev. Drug Discovery* **2002**, *1*, 882−894.

(27) Swann, S. L.; Brown, S. P.; Muchmore, S. W.; Patel, H.; Merta, P.; Locklear, J.; Philip, J.; Hajduk, P. J. A unified, probabilistic framework for structure- and ligand-based virtual screening. *J. Med. Chem.* **2010**, *54*, 1223−1232.

(28) Zhong, S.; Chen, X.; Zhu, X.; Dziegielewska, B.; Bachman, K. E.; Ellenberger, T.; Ballin, J. D.; Wilson, G. M.; Tomkinson, A. E.; MacKerell, A. D., Jr. Identification and validation of human DNA ligase inhibitors using computer-aided drug design. *J. Med. Chem.* **2008**, *51* (15), 4553−4562.

(29) *Sybyl*, version 7.1; Tripos, Inc.: St. Louis, MO, 2005.

(30) Gasteiger, J.; MarioMarsili, M. Iterative partial equalization of orbital electronegativity- a rapid access to atomic charges. *Tetrahedron* **1980**, *36*, 3219−3228.

(31) Jones, G.; Willet, P. GASP: Genetic Algorithm Superimposition Program. In *Pharmacophore Perception, Development, and Use in Drug Design*; Güner, O. F., Ed.; International University Line: La Jolla, CA, 2000; pp 85−106.

(32) Patel, Y.; Gillet, J. V.; Bravi, G.; Leach, R. A. A comparison of the pharmacophore identification programs: Catalyst, DISCO and GASP. *J. Comput.-Aided Mol. Des.* **2002**, *16* (8−9), 653−681.

(33) Olah, M.; Mracec, M.; Ostopovici, L.; Rad, R.; Bora, A.; Hadaruga, N.; Olah, I.; Banda, M.; Simon, Z.; Oprea, T. I. WOMBAT: World of molecular bioactivity. *Chemoinf. Drug Discovery* **2004**, *1*, 223−239.

(34) Tomkinson, A. E.; Chen, X.; Dziegielewska, B.; Mackerell, A. D.; Zhong, S.; Gerald M. Wilson, G. M. Compounds That Inhibit Human DNA Ligases and Methods of Treating Cancer. U.S. Patent Application 12/576,410, filed October 9, 2009.

(35) Sun, D.; Urrabaz, R. Development of non-electrophoretic assay method for DNA ligases and its application to screening of chemical inhibitors of DNA ligase I. *J. Biochem. Biophys. Methods* **2004**, *59* (1), 49−59.

(36) Srivastava, S. K.; Dube, D.; Tewari, N.; Dwivedi, N.; Tripathi, R. P.; Ramachandran, R. Mycobacterium tuberculosis NAD⁺-dependent DNA ligase is selectively inhibited by glycosylamines compared with human DNA ligase I. *Nucleic Acids Res.* **2005**, *33* (22), 7090−7101.

(37) Yang, W. S.; Huang, P.; Plunkett, W.; Becker, F. F.; Chan, Y. J. Dual mode of inhibition of purified DNA ligase I from human cells by 9-beta-D-arabinofuranosyl-2-fluoroadenine triphosphate. *J. Biol. Chem.* **1992**, *267* (4), 2345−2349.

(38) Montecucco, A.; Fontana, M.; Focher, F.; Lestingi, M.; Spadari, S.; Ciarrocchi, G. Specific inhibition of human DNA ligase adenylation by a distamycinderivative possessing antitumor activity. *Nucleic Acid Res.* **1991**, *19* (5), 1067−1072.

(39) Ciarrocchi, G.; Lestingi, M.; Fontana, M.; Spadari, S.; Montecucco, A. Correlation between anthracycline structure and human DNA ligase inhibition. *Biochem. J.* **1991**, *279*, 141−146.

(40) Ciarrocchi, G.; MacPhee, G. D.; Deady, W. L.; Tilley, L. Specific inhibition of the eubacterial DNA ligase by arylamino compounds. *Antimicrob. Agents Chemother.* **1999**, *43* (11), 2766−2772.

(41) Kumar, A.; Siddiqi, M. I. Virtual screening against *Mycobacterium tuberculosis* dihydrofolate reductase: Suggested workflow for compound prioritization using structure interaction fingerprints. *J. Chem. Inf. Model.* **2008**, *27* (4), 476−488.

(42) *Pharmacophore Perception, Development, and Use in Drug Design*; Güner, O. F., Ed.; International University Line: La Jolla, CA, 2000; Vol. 2.

(43) *UNITY, Sybyl*, version 7.1; Tripos, Inc.; St. Louis, MO, 2004.

(44) Lipinski, C. A. Lead-and drug-like compounds: The rule-of-five revolution. *Drug Discovery Today: Technol.* **2004**, *1* (4), 337−341.

(45) Pascal, J. M.; O'Brien, P. J.; Tomkinson, A. E.; Ellenberger, T. Human DNA ligase I completely encircles and partially unwinds nicked DNA. *Nature* **2004**, *25*; *432* (7016), 473−478.

(46) Rarey, M.; Kramer, B.; Lengauer, T.; Klebe, G. A fast flexible docking method using an incremental construction algorithm. *J. Mol. Biol.* **1996**, *261* (3), 470−489.

(47) Kollman, P. A.; Massova, I.; Reyes, C.; Kuhn, B.; Huo, S.; Chong, L.; Lee, M.; Lee, T.; Duan, Y.; Wang, W.; Donini, O.; Cieplak, P.; Srinivasan, J.; Case, D. A.; Cheatham, T. E. Calculating structures and free energies of complex molecules: Combining molecular mechanics and continuum models. *Acc. Chem. Res.* **2000**, *33* (12), 889−897.

(48) Dolinsky, T. J.; Czodrowski, P.; Li, H.; Nielsen, J. E.; Jensen, J. H.; Klebe, G.; Baker, N. A.PDB2PQR: Expanding and upgrading automated preparation of biomolecular structures for molecular simulations. *Nucleic Acids Res.* **2000**, *35*, W522−5.

(49) Barakat, K. H.; Jordheim, L. P.; Perez-Pineiro, R.; Wishart, D.; Dumontet, C.; Tuszynski, J. A. Virtual screening and biological evaluation of inhibitors targeting the XPA-ERCC1 interaction. *PloS One* **2012**, *7* (12), e51329.

(50) Wang, T.; Tomic, S.; Gabdoulline, R. R.; Wade, R. C. How optimal are the binding energetics of barnase and barstar? *Biophys. J.* **2004**, *87* (3), 1618−1630.

(51) Pérez, C.; Pastor, M.; Ortiz, A. R.; Gago, F. Comparative binding energy analysis of HIV-1 protease inhibitors: Incorporation of solvent effects and validation as a powerful tool in receptor-based drug design. *J. Med. Chem.* **1998**, *41* (6), 836−852.

(52) Chen, X.; Pascal, J.; Vijayakumar, S.; Wilson, G. M.; Ellenberger, T.; Tomkinson, A. E. Human DNA ligases I, III and IV − Purification and new specific assays for these enzymes. *Methods Enzymol.* **2006**, *409*, 39−52.

(53) Brown, D. A.; Kharkar, P. S.; Parrington, I.; Maarten, R. EA; Dutta, A. K. Structurally constrained hybrid derivatives containing octahydrobenzo [g or f] quinoline moieties for dopamine D2 and D3 receptors: Binding characterization at D2/D3 receptors and elucidation of a pharmacophore model. *J. Med. Chem.* **2008**, *51* (24), 7806−7819.

(54) Moitessier, N.; Henry, C.; Maigret, B.; Chapleur, Y. Combining pharmacophore search, automated docking, and molecular dynamics simulations as a novel strategy for flexible docking. Proof of concept: Docking of arginine-glycine-aspartic acid-like compounds into the αvβ3 binding site. *J. Med. Chem.* **2004**, *47* (17), 4178−4187.

(55) Hurst, T. Flexible 3D searching: The directed tweak technique. *J. Chem. Inf. Comput. Sci.* **1994**, *34* (1), 190−196.

(56) *Foye's Principles of Medicinal Chemistry*; Lemke, T. L., Williams, D. A., Eds.; Lippincott Williams & Wilkins: Philadelphia, PA, 2008.

(57) Schneider, G.; Böhm, H. J. Virtual screening and fast automated docking methods. *Drug Discovery Today* **2002**, 7 (1), 64−70.